Research Article

Rui Xu, Mingyu Zhang*, Yuyan Zhang and Hongge Jia*

Synthesis of rhodium catalysts with amino acid or triazine as a ligand, as well as its polymerization property of phenylacetylene

https://doi.org/10.1515/hc-2022-0014
received April 19, 2022; accepted June 16, 2022

Abstract: Three novel rhodium complexes, with L-tyrosine (L-Tyr), L-arginine (L-Arg), or 2,4-diamino-6-phenyl-1,3,5-triazine (Dpt) as a ligand, named as [Rh(cod)(L-Tyr)], [Rh(cod)(L-Arg)], and [Rh(cod)(Dpt)$_2$], respectively, had been synthesized for catalyzing the polymerization of phenylacetylene. Their yields were 62.34, 54.87, and 58.21%, respectively, by the most suitable synthesis conditions at 25°C for 4 h. The structures and purity of these complexes were proved by ^{1}H NMR, element analysis, and scanning electron microscope (SEM). It has been examined that phenylacetylene could be polymerized by the three complexes as catalysts with high degrees of polymerization (n = 368, 385, and 664, respectively) and yields (about 87.62, 88.39, and 59.67%, respectively). In conclusion, compared with traditional [Rh–N] type catalysts, the novel [N–Rh–N] type catalyst ([Rh(cod)(Dpt)$_2$]) gained better catalytic performance. By comparing the yield, Mw, and degree of their polymerization, the polymerization mechanism was found under the [N–Rh–N] type rhodium catalyst system.

Keywords: [N–Rh–N] type, rhodium catalyst system, [Rh(cod)(Dpt)$_2$]

1 Introduction

Using catalysts to increase the reaction rate and selectivity was one of the most economical and effective methods in modern industrial production. Because of its high activity, high application, and high regularity, rhodium catalysts have been frequently employed in hydrogenation [1], oxidation [2], hydroformylation [3], oxidative coupling [4], and polymerization of alkynes [5]. Recently, the polymerization of phenylacetylene (PA) became a research hotspot. Therefore, it is of great significance to obtain high-performance polyphenylacetylene by rhodium catalysts.

In 1969, Kern [6] first reported that rhodium catalysts could catalyze the polymerization of PA. Diene ligands (cod, nbd, dcp, and tfb) as precursors of rhodium catalysts were studied by Saeed et al. [7], Furlani et al. [8], Kishimoto et al. [9], Bennett et al. [10], and Roe and Massey [11]. In 2009, Jimenez et al. [12] prepared and characterized a series of cationic complexes [Rh(diene){$Ph_2P(CH_2)_nZ$}][BF_4] containing functional phosphine ligands of the type $Ph_2P(CH_2)_nZ$ (n = 2 or 3; Z = OMe, NMe_2 or SMe). The ligands were screened and optimized to obtain better catalytic activity for the polymerization of PA. Angoy et al. [13] synthesized the dinuclear [Rh_2(diene){μ-$NH(CH_2)_3PPh_2$}$_2$] complexes with π-acceptors diene ligands, which exhibited remarkable catalytic activity in the stereoregular polymerization of PA.

In addition to phosphine ligands, rhodium catalysts with nitrogen-containing heterocycle ligands, such as pyridine, porphyrin, quinoline, and amino acid [14–17], were also used for polyphenylacetylene. Pan et al. [14] studied the reaction of self-made methyl-2-butyrate-pyridine (MBP)

*** Corresponding author: Mingyu Zhang,** College of Chemistry and Chemical Engineering, Heilongjiang Province Key Laboratory of Polymeric Composition, Qiqihar University, Wenhua Street 42, Qiqihar, 161006, China, e-mail: zhangmingyuno1@163.com
*** Corresponding author: Hongge Jia,** College of Chemistry and Chemical Engineering, Heilongjiang Province Key Laboratory of Polymeric Composition, Qiqihar University, Wenhua Street 42, Qiqihar, 161006, China, e-mail: jiahongge@qqhru.edu.cn, tel: +86-452-2738752
Rui Xu: College of Chemistry and Chemical Engineering, Heilongjiang Province Key Laboratory of Polymeric Composition, Qiqihar University, Wenhua Street 42, Qiqihar, 161006, China, e-mail: xurui5670@163.com
Yuyan Zhang: College of Chemistry and Chemical Engineering, Heilongjiang Province Key Laboratory of Polymeric Composition, Qiqihar University, Wenhua Street 42, Qiqihar, 161006, China, e-mail: zyy_18814664686@163.com

with $[Rh(CO)_2Cl]_2$ to obtain rhodium catalyst $[Rh(CO)_2(MBP)Cl]$, which was applied to the carbonylation of MeOH to AcOH. Stateman et al. [15] designed the azuliporphyrin ligand by azulene dialdehyde and tripyranes and then obtained the azuliporphyrin rhodium catalyst. Furlani et al. [16] found that rhodium complex with pyridine as a ligand showed high stereoregularity in the polymerization of PA. Kondo et al. [17] reported a catalyst with one 2-methyl-8-quinolinolate ligand (abbreviated to 2-Me-Q) and two –CO ligands on the Z-selective anti-Markovnikov addition of alcohols to terminal alkynes. Zhao et al. [4] synthesized rhodium catalysts with L-phenylalanine, L-valine, and L-proline as ligands and used them to catalyze the oxidative coupling reaction of PA and 2,4-dihydroxybenzaldehyde as substrates to obtain the flavonoid compounds.

In the present study, the novel catalysts, [Rh(cod)(L-Tyr)] (cod = 1,5-cyclooctadiene, L-Tyr = L-tyrosine), [Rh(cod)(L-Arg)] (L-Arg = L-arginine), and $[Rh(cod)(Dpt)_2]$ (Dpt = 2,4-diamino-6-phenyl-1,3,5-triazine), were synthesized, isolated, and purified by recrystallization. Especially, polyphenylacetylene catalyzed by $[Rh(cod)(Dpt)_2]$ had a higher molecular weight and degree of polymerization than that of other catalysts. Based on the polymerization results, it was discussed that the number of intramolecular Rh–N bonds affected the polymerization ability.

2 Results and discussion

Three novel rhodium catalysts with L-Tyr, L-Arg, and Dpt as ligands were synthesized (Scheme 1), namely, [Rh(cod)(L-Tyr)], [Rh(cod)(L-Arg)], and $[Rh(cod)(Dpt)_2]$.

Rhodium catalysts, [Rh(cod)(L-Arg)], [Rh(cod)(L-Tyr)], and $[Rh(cod)(Dpt)_2]$, were successfully prepared in this study. ^1H NMR spectrum of $[Rh(cod)(Dpt)_2]$ is shown in Figure 1. The peaks of e, f, and d correspond to hydrogen absorption on the phenyl ring. a_1, a_2, and b were the absorption peak of hydrogen position in cod. Due to the $–CH_2–$ conformation in cod and test solvent dimethyl sulfoxide (DMSO), the two hydrogen atoms were influenced differently by the coordinate bond of Rh·||, so there were two groups (a_1 and a_2) of split peaks. The broad peak of c showed active hydrogen atoms of $–NH_2$. ^1H NMR spectra of [Rh(cod)(L-Arg)] and [Rh(cod)(L-Tyr)] were given in the supporting information (Figures A1 and A2).

Elemental analysis of the synthesized rhodium catalysts was carried out. The results showed that although there was a little disparity between the measured data and the theoretical value, it could also prove the purity of the products obtained. The SEM images of the three synthesized rhodium catalysts are shown in Figure 2. [Rh(cod)(L-Tyr)] was presented with a loose random pore structure and stacked together (Figure 2a). [Rh(cod)(L-Arg)]

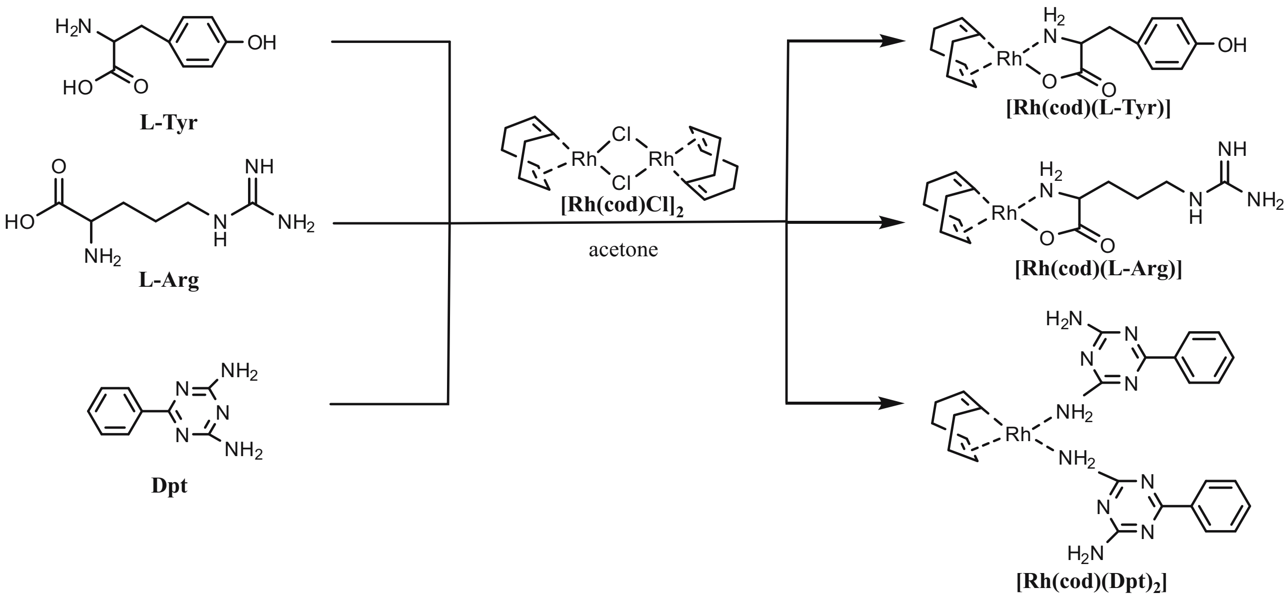

Scheme 1: Synthesis of rhodium catalysts.

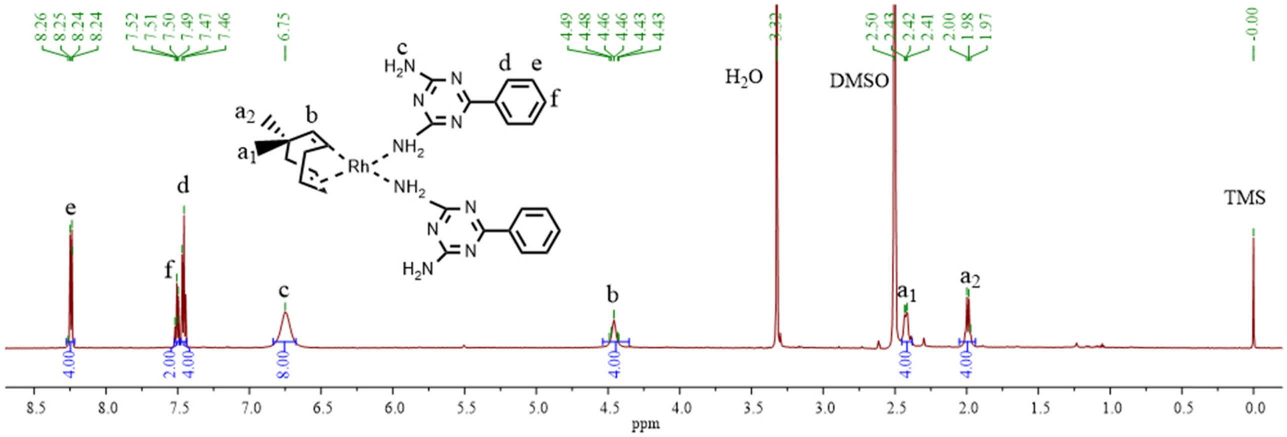

Figure 1: ^{1}H NMR spectrum of [Rh(cod)(Dpt)$_2$] in DMSO.

was a lamellar structure (Figure 2b). [Rh(cod)(Dpt)$_2$] presented a serried honeycomb structure (Figure 2c), which was stable, with a large specific surface area and many catalytic sites. It also manifested high purity. Image-D showed smaller gaps at 100 times, which proved a result of the strong π–π stacking interaction because of the triazine and phenyl ring in [Rh(cod)(Dpt)$_2$].

After determining the structures of novel catalysts, the influence of yield by reaction conditions was paid more attention. In addition to the factors of the catalysts, reaction time and temperature also had a certain impact on the reaction process (Table 1). By adjusting the reaction time and temperature, the optimum was obtained at 25°C for 4 h, namely, [Rh(cod)(L-Tyr)] (62.34%), [Rh(cod)(L-Arg)] (54.87%), and [Rh(cod)(Dpt)$_2$] (58.21%). Due to the shorter reaction time (for 2 h in No. 1, 6, and 11 in Table 1) or lower temperature (at 10°C in No. 4, 9, and 14 in Table 1), the yields decreased, which may be because the reaction was carried out incompletely.

Conversely, the longer reaction time (for 6 h in No. 3, 8, and 13 in Table 1) also caused the yields decreased, which may because of side reactions, such as decomposition

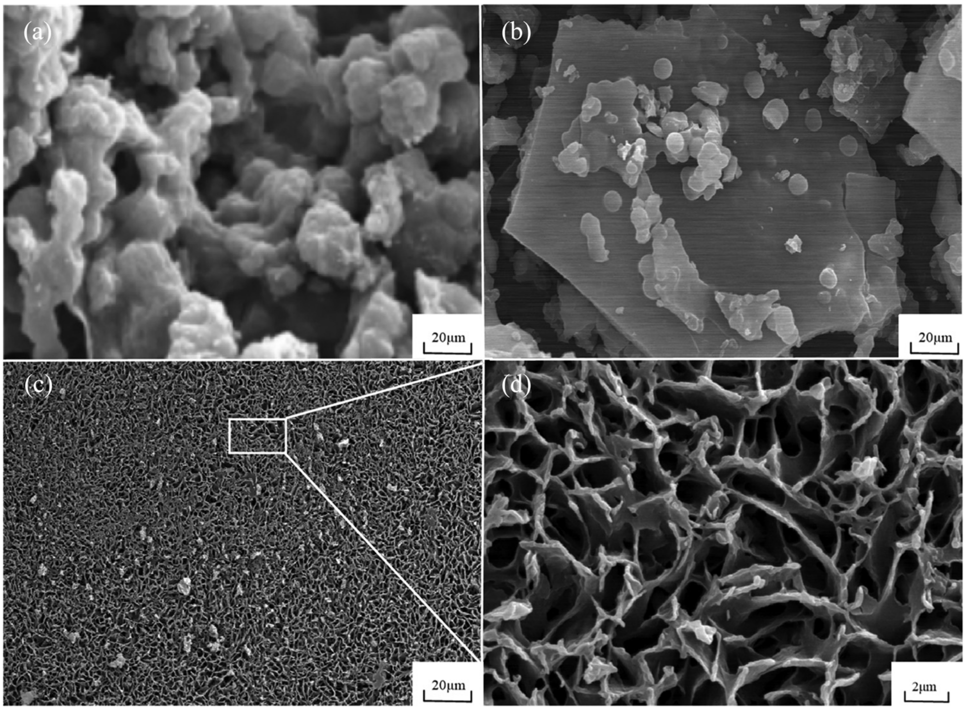

Figure 2: SEM images of the rhodium catalysts: (a) [Rh(cod)(L-Tyr)]; (b) [Rh(cod)(L-Arg)]; (c) [Rh(cod)(Dpt)$_2$]; and (d) enlarged 100 times of image-C.

Table 1: The yields of catalysts under different reaction times and temperature

No.	Catalyst	Time (h)	Temperature (°C)	Yield (%)
1	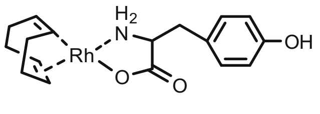 [Rh(cod)(L-Tyr)]	2	25	13.52
2	[Rh(cod)(L-Tyr)]	4	25	62.34
3		6	25	58.19
4		4	10	20.43
5		4	40	60.82
6	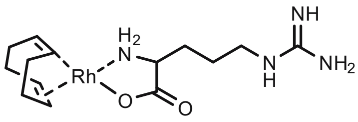 [Rh(cod)(L-Arg)]	2	25	26.44
7	[Rh(cod)(L-Arg)]	4	25	54.87
8		6	25	54.17
9		4	10	18.52
10		4	40	52.14
11	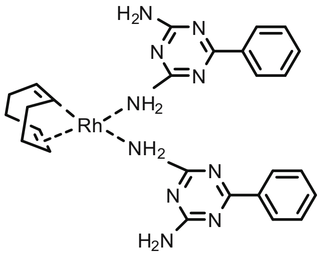 [Rh(cod)(Dpt)2]	2	25	27.36
12	[Rh(cod)(Dpt)$_2$]	4	25	58.21
13		6	25	53.64
14		4	10	19.47
15		4	40	57.32

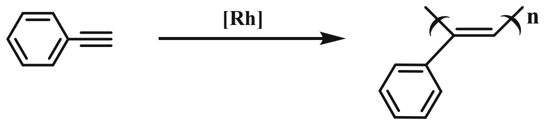

PA **PPA**

[Rh]: [Rh(cod)(L-Tyr)], [Rh(cod)(L-Arg)] or [Rh(cod)(Dpt)$_2$]

Scheme 2: Polymerization of phenylacetylene.

of products. Therefore, it was believed that 4 h and 25°C were the best reaction conditions for the synthesis.

For detecting the catalytic polymerization property of the novel rhodium catalysts (Scheme 2), they were used to catalyze the polymerization of PA for 4 h at 25°C in different organic solvents (Table 2).

To compare the four organic solvents in Table 2, toluene was most suitable for the polymerization of PA. No matter which catalysts were used, the yields (87.62, 88.39, and 59.67%), the molecular weights (8.83×10^4, 9.55×10^4, and 16.01×10^4), and degrees of polymerization ($n = 368$, 385, and 664) were largest. The reasoning for toluene suitability was due to the similarity of the phenyl ring in toluene solvent and PA, which caused π–π stacking interaction to improve the regularity of the reaction system so that the catalysts could easily capture PA molecules and initiate free radical polymerization. Therefore, polyphenylacetylene (PPA) obtained under toluene had a higher yield, larger molecular weight, and degree of polymerization than those under other solvents. However, degree of polymerization (PD) (always ≈ 2.00) was given little effect in different solvents.

Table 2: Polymerization of PA by three novel rhodium catalysts in different solvents[a]

No.	Catalyst	Solvent	Yield (%)	M_w[b] ($\times10^4$)	PD[b]	*n*[c]
1	[Rh(cod)(L-Tyr)]	Toluene	87.62	8.83	2.35	368
2		Acetone	25.07	3.33	2.17	150
3		DMAC	51.42	4.44	1.93	225
4		THF	14.12	3.43	2.07	162
5	[Rh(cod)(L-Arg)]	Toluene	88.39	9.55	2.43	385
6		Acetone	30.24	5.18	1.89	268
7		DMAC	40.16	3.10	2.32	131
8		THF	32.38	2.87	1.97	143
9	[Rh(cod)(Dpt)$_2$]	Toluene	59.67	16.01	2.36	664
10		Acetone	40.14	5.97	1.86	314
11		DMAC	37.36	6.55	1.95	329
12		THF	29.32	5.13	2.12	237

DMAC: *N,N*-Dimethylacetamide; THF: Tetrahydrofuran.
[a] [PA] = 0.01 mmol/L, [PA]/[Rh] = 100; at 25°C for 4 h.
[b] Determined by gel permeation chromatography (GPC) in THF.
[c] Degree of polymerization, $n = M_n/M_{PA} = (M_w/PD)/M_{PA}$.

Viewed from the catalysts, there were opposite polymerization results in the same toluene solution. For No. 1 and 5 in Table 2, the yields of PPA were both above 87%, the molecular weights were both about 90,000, and the degrees of polymerization were both higher than 350. Conversely, for No. 9, the yield of PPA was under 60%, while the molecular weight was up to 160,000, and degree of polymerization was up to 664.

This brings a question: When choosing [Rh(cod)(Dpt)$_2$] as the catalyst, why the yield of PPA was only about 2/3 as them under the other two, however, the molecular weight and degree of polymerization of PPA were nearly two times? It was because the catalytic mechanism of [N–Rh–N] type catalyst (as shown Scheme 3) was different from that of [Rh–N] type [5].

In the polymerization process, **2** was formed by the rhodium atom in **1** coordinate with one PA molecule. Then, the PA in **2** was restructured and produced a carbon-free radical as **3**. Due to a PA–molecule couple

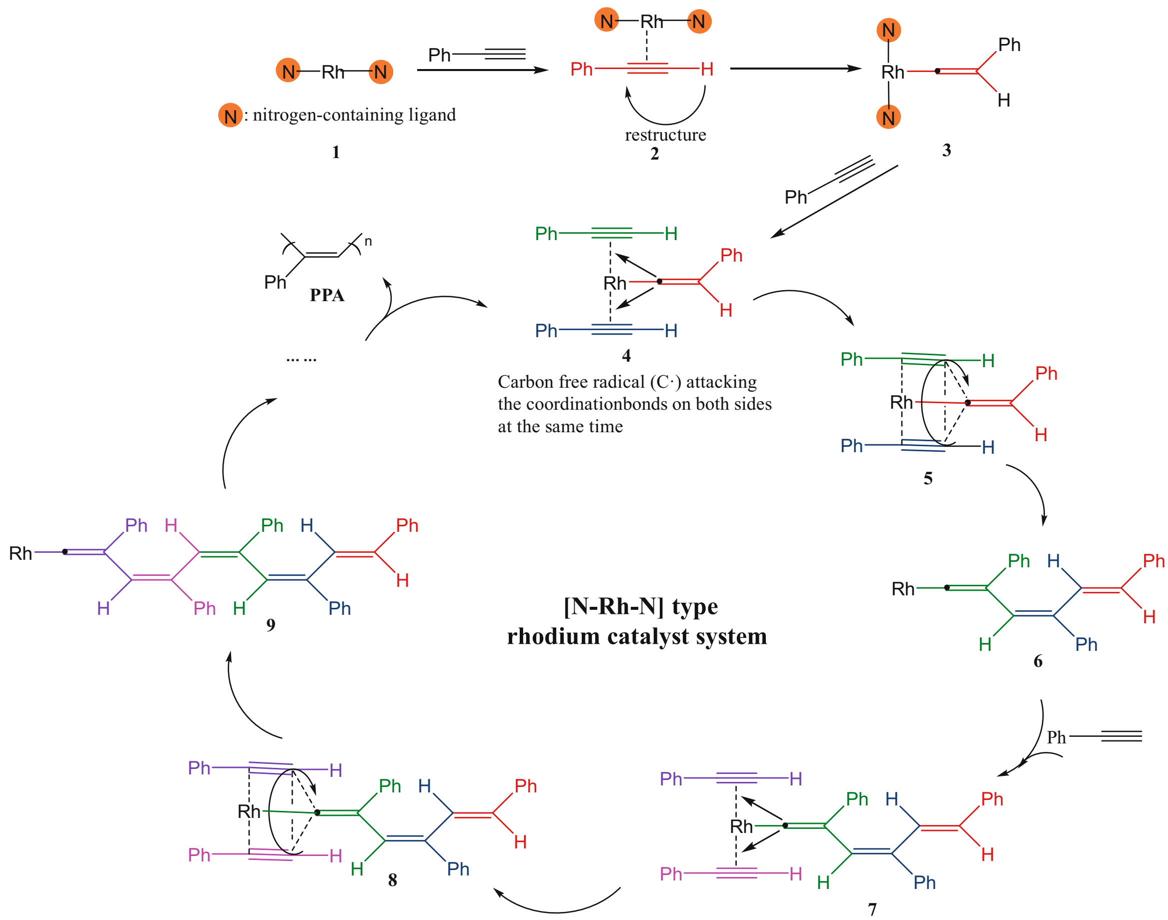

Scheme 3: Polymerization mechanism of PA under [N–Rh–N] type rhodium catalyst system.

replacing the nitrogen ligands in **3** to get **4**, the carbon-free radical (C·) in **4** attacked the coordination bonds on both sides concurrently as **5**. The two PA molecules were inserted and polymerized into the interior. In addition, α-C· was reserved as **6**. Similarly, as the PA–molecule couples joined in the reaction on until the activity of carbon-free radical was too weak to support the subsequent reaction, the PPA macromolecule emerged out of the system. The residue backed to the state of **4** and entered another circle. It was worth mentioning that the double coordination pattern between carbon free radical and two PA molecules kept the activity of carbon-free radical for a longer time, leading to a larger molecular weight and degree of polymerization for PPA.

3 Conclusion

To sum up, three novel rhodium catalysts were successfully synthesized, [Rh(cod)(L-Tyr)], [Rh(cod)(L-Arg)], and [Rh(cod)$(Dpt)_2$]. The amount of text results analysis showed that the best synthesis condition of them was at 25°C for 4 h, and the best polymerization condition of PA catalyzed by using them was in toluene at 25°C for 4 h. Furthermore, due to the particularity of the yield, molecular weight, and degree of polymerization for PPA polymerized from the [N–Rh–N] catalytic system, a new polymerization mechanism of PA was proposed by using [N–Rh–N]-type rhodium catalyst ([Rh(cod)$(Dpt)_2$]. This pattern of *N*-dicoordination was rare. It allowed polymerization simultaneous on both sides of core Rh to obtain a higher degree of polymerization.

4 Experimental

4.1 Materials and equipment

All solvents were dried using standard methods. $RhCl_3{\cdot}3H_2O$, 1,5-cyclooctadiene (cod), L-amino acids, 2,4-diamino-6-phenyl-1,3,5-triazine (Dpt), and PA were purchased from Aladdin Reagent (Shanghai) Co., Ltd. The molecular structures of catalysts were determined by ^1H NMR (600 MHz, Bruker, Germany). Elemental analysis was recorded by PE2400 SERIES II CHNS/O (PerkinElmer, USA) instrument. SEM images were shown with S-4300 (Hitachi, Tokyo, Japan) apparatus. The molecular weight of the polymers was measured by GPC (Polymer Laboratory, UK).

[Rh(cod)Cl]$_2$: This compound was synthesized and purified according to ref. [18].

[Rh(cod)(L-Tyr)]: At nitrogen atmosphere, the solution of L-Tyr (0.0456 mmol, 17.82 mg) and NaOH (0.130 mmol, 5.30 mg) in H_2O (0.60 mL) was added to the suspension of $[Rh(cod)Cl]_2$ (0.0593 mmol, 29.23 mg) in acetone (2.00 mL). The obtained clear yellow solution was stirred for 4 h at 25°C. After filtration, the filtrate was cooled at 5°C until precipitation out from CH_2Cl_2 (2.00 mL), and then sediment was separated and dried to obtain the product as a yellow powder (yield = 62.34%). ^1H NMR (600 MHz, DMSO-d_6) (See Figure A1): 7.03 (d, 2H, J = 12 Hz, CH_2Ph-2,6-H_2), 6.72 (d, 2H, J = 6 Hz, CH_2Ph-3,5-H_2), 4.29 (m, 4H, = CH), 3.80 (s, 2H, NH_2), 3.26 (m, 1H, NHCH), 2.88&2.73 (ds, 2H, Ph-CH_2), 2.22 (t, 4H, J = 6 Hz, cod-CH_2(in)), 1.60 (t, 4H, J = 6 Hz, cod-CH_2(out)). Elemental analyses for $C_{17}H_{22}NO_3Rh$: C, 52.19; H, 5.67; N, 3.58; O, 12.27. Found: C, 52.51; H, 5.27; N, 3.82; O, 12.61 (purity = 92.95%).

[Rh(cod)(L-Arg)]: It was prepared and purified by the similar method as that of Rh(cod)(L-Tyr). Yellow powder (yield = 54.87%). ^1H NMR (600 MHz, $CDCl_3$) (see Figure A2): 7.09 (m, 1H, NH_2NH), 6.72 (d, 2H, J = 12 Hz, NH_2), 4.77 (m, 4H, = CH), 3.49 (m, 1H, COCH_2), 2.10 (m, 2H, NHCH_2), 1.25 (m, 8H, cod-CH_2), 0.89 (m, 4H, CHCH_2CH_2CH_2). Elemental analyses for $C_{14}H_{24}N_4O_2Rh$: C, 43.87; H, 6.31; N, 14.62; O, 8.35. Found: C, 43.96; H, 6.53; N, 14.42; O, 8.26 (purity = 96.63%).

[Rh(cod)(Dpt)$_2$]: It was also prepared and purified by a similar method as that of Rh(cod)(L-Tyr). Yellow powder (yield = 58.21%). ^1H NMR (600 MHz, DMSO-d_6) (see Figure 1): 8.25 (q, 4H, J = 6 Hz, Ph-3,5-H_2), 7.52 (q, 2H, J = 6 Hz, Ph-4-H), 7.46 (t, 4H, J = 12 Hz, Ph-2,6-H_2), 6.75 (s, 8H, NH_2), 4.46 (m, 4H, = CH), 2.43 (t, 4H, J = 6 Hz, cod-CH_2(in)), 1.98 (t, 4H, J = 6 Hz, cod-CH_2(out)). Elemental analyses for $C_{26}H_{30}N_{10}Rh$: C, 53.34; H, 5.16; N, 23.92. Found: C, 53.62; H, 5.13; N, 24.11 (purity = 99.21%).

Funding information: This work was supported by Heilongjiang Provincial Natural Science Foundation of China (LH2019B032), Heilongjiang Provincial Leading Talent Echelon Infrastructure funds (2019-278), China, and The Fundamental Research Funds in Heilongjiang Provincial Universities (No: 135309503).

Conflict of interest: Authors state no conflict of interest.

Data availability statement: The datasets generated during and/or analyzed during the current study are available from the corresponding author on reasonable request.

References

[1] Sanchez A, Fang MF, Ahmed A, Sanchez-Delgado RA. Hydrogenation of arenes, *N*-heteroaromatic compounds, and alkenes catalyzed by rhodium nanoparticles supported on magnesium oxide. Appl Catal A: Gen. 2014;447:117–24.

[2] Mimoun H, Machirant M, Roch IS. Activation of molecular oxygen: Rhodium-catalyzed oxidation of olefins. J Am Chem Soc. 1978;100:5437–44.

[3] Yang J. Rhodium phosphine complex catalyzed hydroformylation of FCC light gasoline olefins. Qingdao: China University of Petroleum; 2018. p. 2–50.

[4] Zhao XY, Jia HG, Song HM. Oxidation coupling of benzylene with 2,4-hydroxybenzaldehyde over rhodium catalyst with Amino acid as ligand. Chem Res. 2020;31:32–4.

[5] Ke ZF, Abe S, Ueno T, Morokuma K. Rh-catalyzed polymerization of phenylacetylene: theoretical studies of the reaction mechanism, regioselectivity, and stereoregularity. J Am Chem Soc. 2011;133:7926–41.

[6] Kern RJ. Preparation and properties of isomeric polyphenylacetylenes. J Polym Sci Part A-I: Polym Chem. 1969;7:621–31.

[7] Saeed I, Shiotsuki M, Masuda T. Effect of diene ligands in the rhodium-catalyzed polymerization of phenylacetylene. Macromolecules. 2006;39:8977–81.

[8] Furlani A, Napoletano C, Russo MV, Camus A, Marsich N. The influence of the ligands on the catalytic activity of a series of Rh (I) complexes in reactions with phenylacetylene: Synthesis of stereoregular poly (phenyl) acetylene. J Polym Sci Part A: Polym Chem. 1989;27:75–86.

[9] Kishimoto Y, Itou M, Miyatake T, Ikariya T, Noyori R. Polymerization of monosubstituted acetylenes with a zwitterionic rhodium (I) complex, Rh $^+$ (2,5-norbornadiene)[(η6-C_6H_5) B–$(C_6H_5)_3$]. Macromolecules. 1995;28:6662–6.

[10] Bennett MA, McMahon IJ, Pelling S, Robertson GB, Wickramasinghe WA. Protonation of dicyclopentadiene complexes of ruthenium (0), osmium (0), rhodium (I), and iridium (I). Single-crystal X-ray study of [Os (2,3,5-η-C10H13) (η-C6H3Me3-1,3,5)] PF6, a complex containing an Os-H-C interaction. Organometallics. 1985;4:754–61.

[11] Roe DM, Massey AG. Perfluorophenyl derivatives of the elements XXVI. Tetrafluorobenzobarrelene complexes of Mn, Co, Rh, Pd and Pt. J Organomet Chem. 1971;28:273–9.

[12] Jimenez MV, Perez-Torrente JJ, Bartolome MI, Vispe E, Lahoz FJ, Oro LA. Cationic rhodium complexes with hemilabile phosphine ligands as polymerization catalyst for high molecular weight stereoregular poly (phenylacetylene). Macromolecules. 2009;42:8146–56.

[13] Angoy M, Jimenez MV, Orduna PG, Oro LA, Vispe E, Perez-Torrente JJ. Dinuclear phosphine-amido $[Rh_2(\text{diene})\{\mu\text{-}NH(CH_2)_3PPh_2\}_2]$ complexes as efficient catalyst precursors for phenylacetylene polymerization. Organometallics. 2019;38:1991–2006.

[14] Pan PL, Liu ZY, Huang MK, Yuan GQ. Synthesis and properties of rhodium complexes with cis dicarbonyl methyl 2-butyrate pyridine. Chem Bull. 1995;7:34–5.

[15] Stateman LM, Ferrence GM, Lash TD. Rhodium (III) azuliporphyrins. Organometallics. 2015;45:3842–8.

[16] Furlani A, Napoletano C, Russo MV, Feast WJ. Stereoregular polyphenylacetylene. Polym Bull. 1986;16:311–7.

[17] Kondo M, Kochi T, Kakiuchi F. Rhodium-catalyzed anti-markovnikov intermolecular hydroalkoxylation of terminal acetylenes. J Am Chem Soc. 2011;133:32–4.

[18] Paiaro G, Musco L, Diana G. Chemical and structural characterization of some π-allylicderivatives of rhodium (III). J Organomet Chem. 1965;4:466–74.

Appendix

It was worth mentioning that –CH_2– of cod produced two groups of split peaks in DMSO solution, which is inexistent in $CDCl_3$.

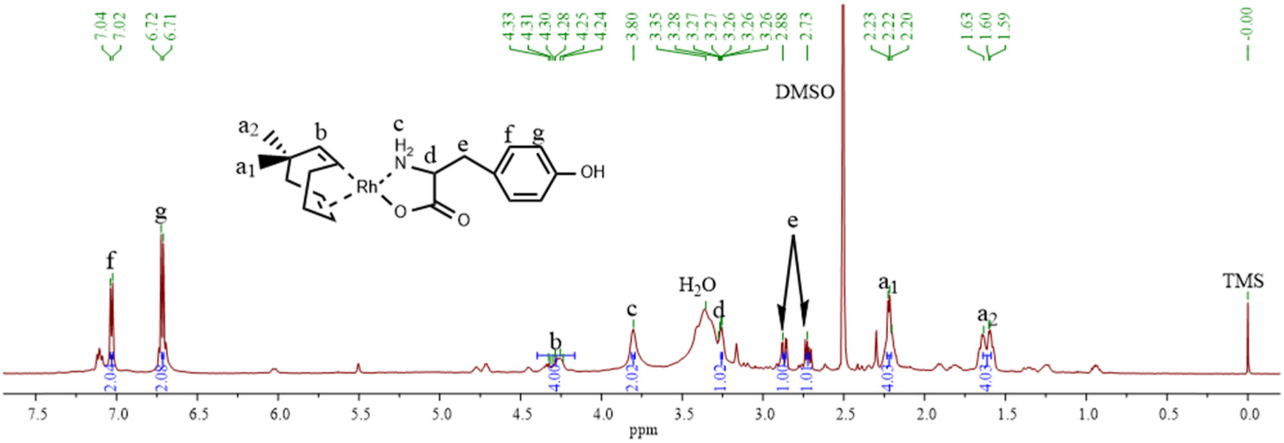

Figure A1: ^{1}H NMR spectrum of [Rh(cod)(L-Tyr)] in DMSO.

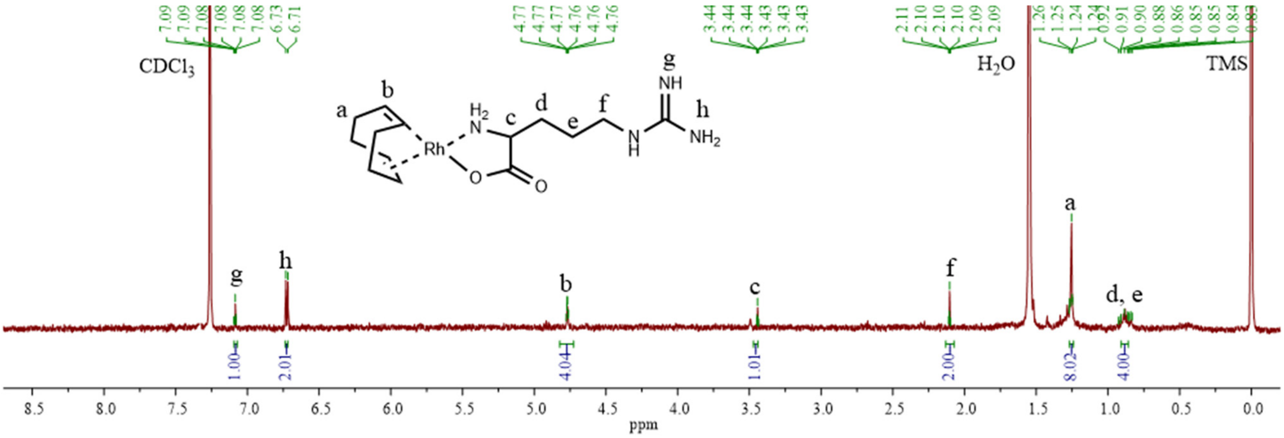

Figure A2: ^{1}H NMR spectrum of [Rh(cod)(L-Arg)] in $CDCl_3$.